processes

MDPI

Article

Screening and Evaluation of Anti-Salt Surfactant/Polymer System for Enhanced Oil Recovery in a Low-Permeability Reservoir in Changqing Oilfield, China

Yangnan Shangguan [1,2], Xuefeng Qu [1,2], Guowei Yuan [1,2], Weiliang Xiong [1,2], Kang Tang [1,2], Qianqian Tian [1,2], Lei Liu [1,2], Hua Guan [1,2], Qi Wang [1,2], Xingmei Kang [1,2], Lizhi Cheng [3] and Hongda Hao [3,*]

[1] Exploration & Development Research Institute, Changqing Oilfield Company, Xi'an 710021, China
[2] National Engineering Laboratory for Exploration and Development of Low-Permeability Oil & Gas Fields, Xi'an 710021, China
[3] School of Petroleum and Natural Gas Engineering, School of Energy, Changzhou University, Changzhou 213164, China
* Correspondence: haohongda90@126.com

Abstract

A low-permeability, high salinity reservoir entered the high-water-cut and high recovery degree stage in the middle and late stages of development, and it is difficult to tap the potential of water flooding. The overall water flooding recovery of the developed low-permeability reservoir is low, and the produced water has high oil content, many granular impurities, and high inorganic salt content. The polymer–surfactant binary system was studied according to the reservoir conditions. The polymer acrylic acid/polyacrylamide/2-acryloylamino-2-methyl-1-propanesulfonic acid was selected by viscosity measurement. The viscosity stability of the polymer and the effect of the flooding system were evaluated, and the salt-tolerant surfactant sulfonated betaine + amides and coco composite system were screened, and the viscosity, interfacial tension, and displacement effect were evaluated. Finally, the polymer–surfactant binary flooding system was formed. The system has good compatibility, the interfacial tension can still be reduced to 10^{-3} mN/m at 40 °C and 23,800 mg/L, and the viscosity of the polymer solution increased by 5.8% upon addition of the surfactant. The composite system can improve the oil displacement efficiency by 21.19%. The results of a parallel core displacement experiment with a 3.91 permeability ratio show that the oil displacement efficiency can be improved by 19.96%. The system has good performance in low-permeability oilfields and can effectively displace crude oil, which is of great significance for the displacement of low-permeability heterogeneous reservoirs.

Keywords: low salinity reservoir; salt-tolerant polymer; composite drive; enhanced oil recovery

Check for updates

Academic Editor: Youguo Yan

Received: 4 December 2025
Revised: 16 January 2026
Accepted: 20 January 2026
Published: 24 January 2026

Copyright: © 2026 by the authors. Licensee MDPI, Basel, Switzerland. This article is an open access article distributed under the terms and conditions of the Creative Commons Attribution (CC BY) license.

1. Introduction

A low-permeability reservoir refers to an oil and gas reservoir where the rock porosity is low and the permeability is less than 50 millidarcies (mD) [1]. Globally, there are huge reserves of low-permeability reservoirs with rich oil and gas resources. Oil-producing countries such as the United States, Russia, and Canada have discovered a large number of low-permeability oil fields [2,3]. For example, the Ventura Oil Field in the United States has a recoverable reserve of 1×10^8 tons, and the Pembina Oil Field in Canada has a geological reserve of 11×10^8 tons and a recoverable reserve of 3×10^8 tons. It is estimated that low-permeability oil reservoir resources account for more than about 30% of the total known

 https://doi.org/10.3390/pr14030408

petroleum resources [4,5]. In China, the proven reserves of low-permeability reservoirs account for more than 65%. In Chinese oil and gas basins, Paleozoic cratonic basins, Mesozoic–Cenozoic faulted basins, and foreland basins are the main distribution areas of low-permeability reservoirs, collectively making up 85% of the country's oil and gas reserves [6,7].

With the gradual development of high-water-cut oilfields and resource consumption, low-permeability oilfields have become the focus and difficulty of current oilfield development. However, due to the uneven distribution of reservoir properties, low-permeability reservoirs suffer from the problem of reservoir heterogeneity [8,9]. Reservoir heterogeneity leads to uneven flow direction of injected media, resulting in extremely uneven permeability distribution of the injected fluid in the reservoir. Water molecules move at a slower speed in the reservoir, and the economically effective physical driving force is small, causing increased costs and reduced efficiency, which seriously affects the water-flooding development effect [10,11].

After water flooding, gas injection has become a new method to improve recovery efficiency, among which CO_2 flooding is the most widely applied. In the North American region, the crude oil produced based on CO_2 flooding technology has approached 1.3×10^9 tons [12]. In China, indoor CO_2 flooding experiments and small-scale pilot tests have been successively conducted in Daqing Oilfield, Jilin Oilfield, Jiangsu Oilfield, Shengli Oilfield, and other places. The exploration of the mechanism of CO_2 oil displacement mainly includes the interaction between CO_2 and crude oil [13], CO_2 permeation and diffusion [14], CO_2 dissolution, crude oil displacement, and permeability [15]. CO_2-altering rock wettability and pore-scale mechanisms, and simulation methods as well as molecular dynamics have been researched [16,17]. Although CO_2 flooding is applicable to ultra-low-permeability reservoirs, it is limited in large-scale application due to scarce gas sources and high miscibility pressure.

Furthermore, the scientific application of tertiary oil recovery chemical flooding technology has undoubtedly opened up a new era for the improvement of oil recovery efficiency. Studies have shown that [18], in the global chemical flooding enhanced oil recovery test projects, more than 77% are polymer flooding and nearly 23% are composite systems composed of polymers and surfactants and other chemical substances. Polymer flooding mainly depends on increasing the viscosity of the water phase and reducing the mobility ratio. At present, the traditional polyacrylamide polymer has poor adaptability and cannot adapt to a high-salt, high-temperature reservoir environment [19,20]. In order to improve the oil displacement effect of the polymer, the viscosity of the polymer can be increased by changing its molecular weight. By introducing heat-resistant and salt-tolerant functional monomers into the molecular structure [21], a polymer with hydrophobic association was synthesized [22]. In order to enhance the heat and salt resistance of the polymer, the hyperbranched structure is used to improve the shear resistance of the polymer [23]. Some scholars have also optimized and explained the polymer through viscoelasticity and other aspects [24].

Surfactant flooding is used to improve oil recovery, generally through the following aspects: the low interfacial tension reduces the capillary force, thereby reducing the adhesion force, so as to improve the oil displacement efficiency [25]. Due to the strong emulsifying ability of the surfactant, this can make the crude oil in the pore disperse, resulting in a stripping phenomenon, and contact with the crude oil in the pore and shear emulsification then form a certain particle size of the emulsion droplets [26]. Another method is to destroy the oil film on the rock surface, reduce the adhesion work, and reduce the capillary resistance, forcing the crude oil attached to the rock surface to peel off, thereby improving the oil washing efficiency [27].

At present, the research on chemical flooding in low-permeability reservoirs is relatively comprehensive. However, at present, the cost of polymers and surfactant is high, the treatment of produced liquid is difficult, and there are some problems such as formation adsorption, high cost, and poor adaptability to complex formation conditions [28,29].

Using polymer viscosity to reduce the oil–water mobility ratio, combined with the ability of surfactant to reduce oil–water interfacial tension, coupled with the synergistic effect of alkali and crude oil reaction, ASP flooding shows great potential. Scholars have studied formula synthesis [30,31], chemical bonding within the system [32], and flow model [33]. As the ceiling of the technical performance of chemical flooding, ASP flooding can improve the recovery rate by more than 20% in the ultra-high-water-cut oilfield with a water cut of 98% by virtue of the synergistic effect of the alkali–surfactant–polymer. However, the strong alkali formula can easily cause permanent damage to the formation, and the treatment of the produced fluid is difficult to obtain on a large scale and at low cost.

The alkali-free SP system can well avoid the damage of alkaline substances to the formation. However, due to the shortcomings of poor salt resistance and the sheer resistance of surfactants and unscientific injection methods, the improvement of SP flooding recovery is greatly limited. Furthermore, the Oryx Energies energy company and Shell Petroleum company of the United States carried out field pilot tests of binary composite flooding. The test results show that the binary composite flooding layer also has a good effect on improving oil recovery. Professor Kwak et al. synthesized a new polymer–surfactant binary system whose displacement effect in laboratory tests is close to that of ASP flooding. A large number of scholars' research on the new SP system has greatly compensated for the impact of the lack of alkaline substances [34].

In recent years, whether from field applications in Ranger Oilfield [35], Wilmington Field [36], and oilfields in China [37], indoor experiments [38,39], or simulation experiment results [40], all have demonstrated advantages such as good input–output prospects and great development potential.

The Changqing Oilfield has extremely special geological conditions, belonging to a typical 'three-lows' oil and gas reservoir, namely low porosity, low permeability, and low productivity. Such reservoirs have fine pore structures, extremely low permeability, and are extremely difficult to develop [41]. Long-term reliance on large-scale water injection and fracturing technologies has been employed to improve reservoir seepage conditions. This has resulted in the formation of a complex fracture network in the formation, leading to a severe imbalance in the underground pressure system and extremely strong heterogeneity [42]. Therefore, it is necessary to develop a new extraction chemical agent system through innovative technologies. This paper focuses on the low-permeability reservoir fluid of a certain Changqing Oilfield, using reservoir-produced water for preparation. Through performance evaluation and displacement experiments, low-molecular-weight, salt-tolerant polymers and strong emulsifying surfactants are selected to form a polymer–surfactant binary system, providing strong support for the rational and efficient development of oilfields.

2. Experiments

2.1. Experimental Reagents and Instruments

2.1.1. Experimental Equipment

A Brinell viscometer (Shanghai Qihao Instrument Co., Ltd., Shanghai, China), water bath heater (Shanghai Weichuan Precision Instrument Co., Ltd., Shanghai, China.), and rotor were used for polymer viscosity measurement (Xi'an Automation Instrument Factory No.1, Xi'an, China); a multi-stage membrane holder and micro displacement pump were used for the determination of filtration characteristics (Hai'an Petroleum Research

Instrument Co., Ltd., Haian, China); a precision pressure gauge, parallel water/polymer solution intermediate container, electronic balance, incubator, pressure sensor, core holder, and ring pressure pump were used for resistance testing and displacement experimentation (Shanghai Yiheng Scientific Instrument Co., Ltd., Shanghai, China); an interfacial tension meter, syringe, and sample tube were used to measure the interfacial tension (Shanghai Aifes Precision Instrument Co., Ltd., Shanghai, China); and calibrating tubes, beakers, and test tube racks were used to measure emulsifying properties (Shu Niu Glass Instrument Co., Ltd., Sichuan, China).

2.1.2. Experimental Materials and Reagents

The types of polymers used in the experiment are shown in Table 1. The polymer reagent used in the experiment is from Shanghai Macklin Biochemical Co., Ltd., Shanghai, China.

Table 1. Polymers used in the screening experiments.

Number	Polymer
1	Xanthan gum
2	Polyacrylamide
3	Partially hydrolyzed polyacrylamide
4	Anionic Polyacrylamide
5	2-Acryloylamino-2-methyl-1-propanesulfonic acid/Acrylonitrile-butadine-styrene/Chromium
6	Diallyl dimethyl ammonium chloride/Acrylamide/2-Acryloylamino-2-methyl-1-propanesulfonic acid
7	Star-shape cationic polyacrylamide
8	Acrylamide/Organotitanium polymer
9	N,N-diethylprop-2-enamide/Polyacrylamide/2-Acryloylamino-2-methyl-1-propanesulfonic acid(AAND-1)
10	Acrylic acid/Polyacrylamide/2-Acryloylamino-2-methyl-1-propanesulfonic acid

The types of surfactant used in the experiment are shown in Table 2. The surfactant reagent used in the experiment is from Nanjing Chemical Reagent Co., Ltd., Nanjing, China.

Table 2. Surfactant used in the screening experiments.

Number	Surfactant
A	Sulfonated Betaine
B	Amides, coco
C	Sodium Laurylsulfate
D	Coconut oil acid diethanolamine
E	Sulfonic acids
F	Lauroylamide Propylbetaine
G	Lauryl betaine
H	AmyI gemini quaternary ammonium salt
I	Cocamidopropyl Betaine
J	Dodecyl dimethyl betaine
K	Dodecyl benzenesulphonic acid
L	Benzenesulfonic acid

An ethanol solution, deionized water, and alumina microfiltration membrane with a pore size of 1–10 μm were used to measure the percolation characteristics. The crude oil viscosity used in the displacement experiment was 2 mPa·s, the salinity water was 24,800 mg/L, and the polymer solution concentration was 2000 mg/L; the length of the artificial and natural cores were 30 cm, and the diameter was 2.5 cm. The basic parameters of the core are shown in Table 3.

Table 3. Core data used in displacement experiments.

Core Number	Permeability (mD)	Pore Volume (cm^3)	Saturated Oil Volume (cm^3)	Porosity (%)	Oil Saturation (%)
1	29.2	5.59	3.65	22.8	65.3
2	29.4	5.52	3.54	22.5	64.2
3	24.1	5.52	3.54	22.5	64.2
4	30.7	5.54	3.58	22.6	64.6
5	20.11	5.56	3.6	22.7	64.8
6	37.38	5.74	3.8	23.4	66.2
7	35.9	5.66	3.72	23.1	65.7
8	140.4	4.61	2.55	18.8	55.3

2.2. Experimental Process and Methods

2.2.1. Determination of Polymer Viscosity

a. According to the viscosity range of SP system, the No. 0 rotor was selected for the experiment.

b. The polymer solution of 2000 mg/L was mixed evenly and placed into a constant temperature water bath, and the temperature was adjusted to 40 °C.

c. The rotation speed was set to 7.34 r/min, instrument measurement was started, and the experimental results were recorded.

d. The rotor was cleaned at the end of the test, and the viscosity of the remaining polymer solution was re-measured according to the above experimental steps.

2.2.2. Determination of Polymer Diafiltration

a. Two pieces of alumina microfiltration membrane were placed into the groove of the gripper, the pad was placed into the sealing ring, and the flange bolt was tightened. Connection pipeline: clear water intermediate container → six-way valve → filter membrane holder inlet → outlet → liquid-receiving container. The incubator was preheated to 40 °C.

b. The water valve was opened, and the micro pump cleaned the pipeline at a flow rate of 5 mL/min for 5–10 min to ensure that the pipeline was free of impurities.

c. Injection of polymer solution: After switching to the intermediate container of polymer solution, the constant pressure mode of the displacement pump was set, and the precision pressure gauge was opened to monitor the pressure fluctuation of the pipeline. A container was used to collect the effluent, and the electronic balance automatically recorded the quality every 30 s. Testing continued until the mass flow rate of the effluent was stable.

d. The gripper was removed, the polymer intercepted by the two-stage filter membrane was collected, the particle size distribution of the original solution was compared with the effluent and intercepts at all levels, and the matching relationship and migration characteristics were evaluated.

2.2.3. Determination of Interfacial Tension

a. The interfacial tensiometer and computer power supply were connected, the temperature was set to 40 °C, the interface tension measurement software was opened, the sample viscosity and related parameters were set, and the sample tube was washed with ethanol and distilled water approximately 2–3 times.

b. The measured external phase solution (water phase) was injected, and about a drop of the internal phase (oil phase) was injected with a syringe.

c. After the instrument reached the set temperature, the sample tube was loaded into the rotating shaft, the clamping cap was tightened, and the observation microscope was adjusted to a suitable position for observation.

d. The motor switch was pressed, the speed was adjusted, the length and diameter of the droplet were measured, and the interfacial tension was calculated by the following formula:

$$\sigma = 4.442 \times 10^9 \Delta\rho P^2 \left(\frac{d}{n}\right)^3 f\left(\frac{L}{d}\right) \quad (1)$$

where, σ is the interfacial tension, $\Delta\rho$ is the density difference between the two phases, P is the rotational speed, n is the refractive index of the outer phase, d is the diameter reading on the instrument, and $f(L/d)$ is the correction factor.

2.2.4. Determination of Surfactant Emulsification

a. Ten mL of surfactant solution and crude oil, respectively, were added to a 25 mL test tube. The tube was covered with the test tube stopper, and each test tube was shaken up and down 30 times.

b. The shaken test tube was immediately placed vertically on the test tube rack, at which point timing began, and the volume of the separated water in the test tube was recorded every 3 min for a total of 30 min.

c. The most stable test tube was shaken 30 times again, and the type of emulsion was determined by dispersion.

d. Emulsification efficiency (*fe*) was calculated using the following formula:

$$fe = \frac{m_0}{m_1} \cdot 100\% \quad (2)$$

where m_0 represents the oil content of the emulsion layer, and m_1 represents the total amount of oil added.

e. Emulsion stability (*Ste*) was calculated using the following formula:

$$ste = \frac{V_0}{V_1} \cdot 100\% \quad (3)$$

where V_0 represents the volume of precipitated water, and V_1 represents the total volume of emulsion.

f. The emulsification comprehensive index (*Sei*) was calculated using the following formula:

$$Sei = k \cdot \sqrt{fe \cdot Ste} \quad (4)$$

where k is the adjustment coefficient, and the value in this paper is 1.

2.2.5. Determination of FR and Recovery Ratio

a. The natural core was selected and vacuumed, formation water was saturated, pore volume and porosity were calculated, and water phase permeability was measured.

b. The core was placed in a thermostat at 40.2 °C to saturate the simulated oil, the saturated oil volume was recorded, and the oil saturation was calculated.

c. The formation water of 1.75 PV was injected at the injection rate of 0.2 mL/min; the oil production, water production, and liquid production were recorded; the displacement pressure difference was recorded; and the water content and recovery rate were calculated.

d. The polymer solution of 0.5 PV was injected at the injection rate of 0.2 mL/min; the oil production, water production, and liquid production were recorded; the displacement pressure difference was recorded; and the water content and recovery rate were calculated.

e. The formation water of 2.4 PV was injected at the injection rate of 0.2 mL/min; the oil production, water production, and liquid production were recorded; and the displacement pressure difference was recorded to calculate the water content and recovery rate.

f. The resistance coefficient was calculated according to the average displacement pressure difference between water flooding and chemical flooding. The degree of enhanced oil recovery by chemical flooding was obtained by the difference between total recovery and water flooding recovery.

2.2.6. Determination of Flow Rate in Parallel Core Displacement Experiment

During the experiment, the liquid production of a high-permeability core and low-permeability core can be recorded as L_h and L_l at the same time. The split rate D_h and D_l of the high-permeability zone and the low-permeability zone can be calculated by using the liquid production. D_h and D_l are shown in Equations (5) and (6), respectively. The displacement effect of heterogeneous cores can be monitored by changes in the flow rate:

$$D_h = \frac{L_h}{L_h + L_l} \tag{5}$$

$$D_l = \frac{L_l}{L_h + L_l} \tag{6}$$

where L_h is the liquid output of the high-permeability zone (mL), L_l is the liquid output of the low-permeability zone (mL), D_h is the diversion rate of the high-permeability zone (%), and D_l is the diversion rate of the low-permeability zone (%).

3. Results and Discussion

3.1. Polymer Performance Evaluation

3.1.1. Salt-Tolerant Polymer Screening

The reservoir of the target block is a medium-pore and medium-throat type, with a median radius of about 1.89 μm. Based on the Flory–Harkins theory and the regression results of measured data [43], considering the matching relationship between polymer molecular weight and core permeability, the polymer molecular weight should be controlled below 10 million. The viscosity of the formation of crude oil in the test area is 2.0 mPa·s, and the viscosity ratio of polymer aqueous solution to the formation of crude oil is approximately 3–5 times that, which is the best. Considering the viscosity loss of wellbore and the process in the injection process is approximately 20–40%, the viscosity of polymer solution prepared on the ground is not less than 20 mPa·s. Ten kinds of low molecular weight polymers were identified by screening low molecular weight polymers suitable for blocks. Most of these polymers have been widely tested and applied as potential applications.

We measured the viscosity of different polymers, and the experimental results are shown in the Table 4. The viscosity of the measured polymers was mostly above 15 mPa·s. Only the number 10(Acrylic acid/Polyacrylamide/2-Acryloylamino-2-methyl-1-propanesulfonic acid) has a molecular weight of 9 million. At the same time, the viscosity was above 20 mPa·s. According to the conditions, the number 10 was selected as the polymer that meets the conditions. The polymer is evaluated below.

Table 4. Polymer viscosity determination screening results.

Polymer	1	2	3	4	5
Molecular weight(W)	900	900	1000	900	900
Viscosity(mPa·s)	17.4	16.4	19.2	18.8	16.1
Polymer	**6**	**7**	**8**	**9**	**10**
Molecular weight(W)	1000	900	1000	900	900
Viscosity(mPa·s)	18.0	18.8	17.2	18.7	21.4

The molecular structure of the polymer is shown in Figure 1. The polymer is synthesized from 69% AM, 23% AMPS, and 8% AA. The salt resistance and thickening ability of the system are enhanced by the internal sulfonic acid group and the amide group, which is suitable for high-salinity reservoirs.

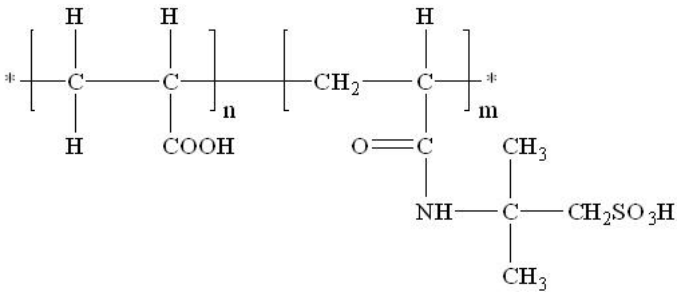

Figure 1. Molecular structure diagram of ternary polymer.

3.1.2. Determination Results of Polymer Viscosity

The selected salt-tolerant polymer was prepared with produced water, and the viscosity of the polymer at different concentrations was measured at 25 °C and 40 °C, respectively. The experimental results are shown in Figure 2. With the increase of polymer concentration, the viscosity of the polymer at different temperatures increases. The viscosity at 40 °C is generally lower than that at room temperature.

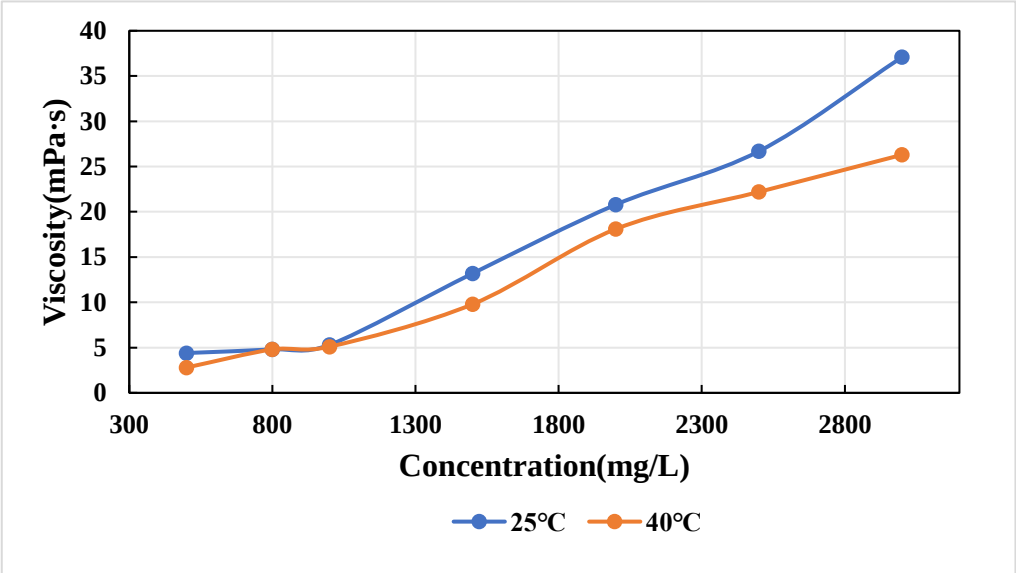

Figure 2. Viscosity measurement results of polymer field produced water at different temperatures and concentrations.

The retention rate of polymer shear viscosity under flow conditions was measured by low permeability core, and the viscosity of injected liquid and produced liquid was measured. The experimental cores are the No. 1 core and the No. 2 core, and the permeability is 29.2 mD and 29.4 mD, respectively. The experimental results are shown in Tables 5 and 6. The viscosity retention rates of the two groups were 96.3% and 98.1%, respectively. The viscosity of the produced water before and after adsorption was measured, and the viscosity retention rate after core adsorption was 94.40%. The experimental results show that the salt-resistant polymer has good viscosity, and the viscosity retention rate after adsorption and shearing is high. According to the viscosity–concentration relationship curve, the reasonable field use concentration of the polymer is 1500–3000 mg/L.

Table 5. Polymer shear viscosity under flow conditions retention rate.

Core Number	Permeability (mD)	Viscosity (mPa·s)		Viscosity Retention Rate (%)
		Injection Liquid	Produced Liquid	
1	29.2	26.7	25.7	96.3
2	29.4	21.3	20.9	98.1

Table 6. Polymer core adsorption viscosity retention rate.

Water Sample	Viscosity Before Adsorption (mPa·s)	Viscosity After Adsorption (mPa·s)	Core Viscosity Retention Rate After Adsorption (%)
Produced water	34	32.1	94.40%

3.1.3. Polymer Diafiltration Determination Results

The determination results are shown in Table 7 below. The results of the polymer filtration factor and viscosity measurement before and after filtration show that the filtration factor (FR) is close to 1.0, indicating that the polymer solution has less impurities, very low suspended particle content, smooth filtration, and will not easily cause formation plugging. Under the conditions of 3 μm and 10 μm membranes, the viscosity retention rate reached more than 81%. The results showed that the salt-resistant polymer had excellent shear resistance and filtration ability, which was suitable for long-distance transportation and deep profile control. It has good filtration characteristics and temperature resistance, and the viscosity retention rate is more than 80% after shearing by porous media.

Table 7. Polymer Filter Factor and Viscosity Measurement Results Before and After Filtration.

Polymer	10 (Acrylic Acid/Polyacrylamide/2-Acryloylamino-2-methyl-1-propanesulfonic Acid)	
Pore size of microporous filter membrane (μm)	3	10
Filtration factor (FR)	1.02	1.02
Retention rate of filter shear viscosity (%)	81.3	82.1

The AA/AMPS/AM copolymer is composed of three functional monomers that have carboxylic acid groups, strong polar sulfonic acid groups, and amide groups, forming the core molecular basis of salt-tolerant oil displacement. The AM flexible segment is used as the molecular skeleton to improve the tensile properties of the copolymer. The carboxylic acid group of AA provides a certain adsorption capacity to enhance the retention effect in the formation pores; the rigid side chain of AMPS maintains the stretchability of the whole molecular chain, and the three form a three-dimensional chain structure, which further strengthens the salt resistance. Compared with traditional polyacrylamide (PAM),

the sulfonic acid group of the AMPS segment will not be like the carboxylic acid group. In the high-salt environment, the charge shielding causes the molecular chain to curl up, and it can always maintain the stretchable spatial conformation and maintain the fluid viscosity, adapt to the high-salt and low-permeability reservoir in Changqing, and have both mobility control and oil washing and production capacity [44,45].

3.1.4. Evaluation of Polymer Displacement Effect

The core displacement experiment was carried out for the polymer system. The density of crude oil is 0.85 g/mL, the salinity of formation water is 24,600 mg/L, the injection water of water flooding is formation water, the chemical flooding is 0.20% polymer formation water solution, the experimental temperature is 40 °C, and the injection rate is 0.05 mL/min. The experimental cores are the No. 3 core and the No. 4 core, and the permeability is 29.2 mD and 29.4 mD, respectively. The experimental results are shown in Figures 3 and 4.

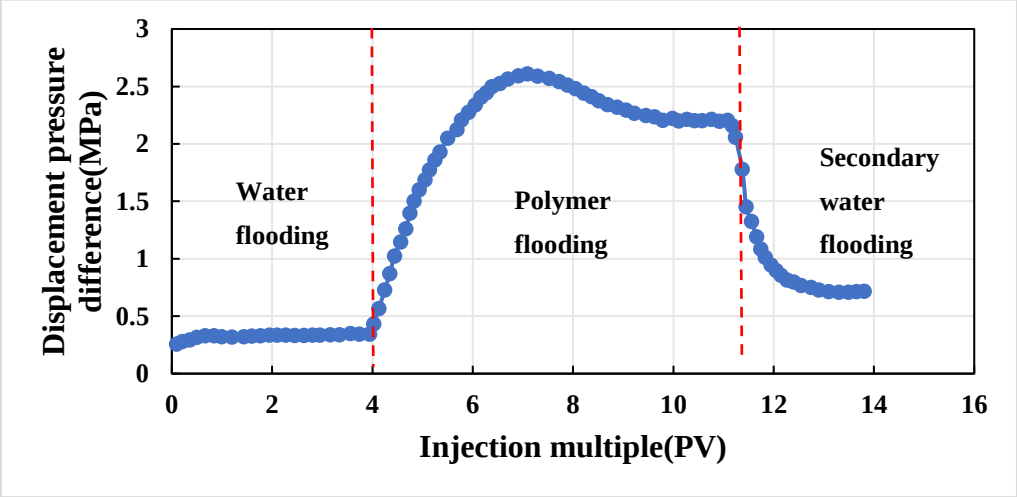

Figure 3. Results of artificial core displacement experiments.

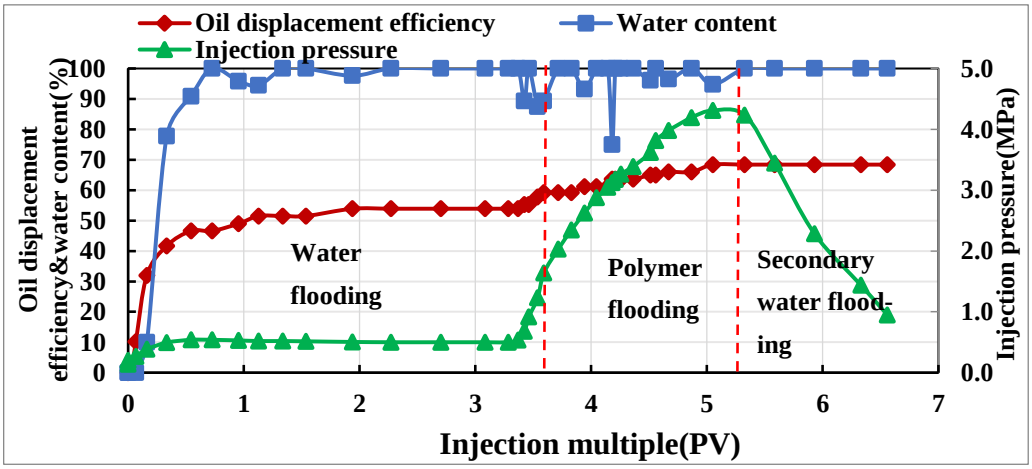

Figure 4. Results of natural core oil displacement experiments.

Salt-tolerant polymers can be effectively injected into low-permeability cores, showing good fluidity and stability. Their resistance coefficient is as high as 18.0, showing excellent deep profile control potential. The residual resistance coefficient is 4.4, which is in a reasonable range. In the natural core experiment, polymer flooding increased the oil displacement efficiency from 53.9% to 68.4%, with an increase of 14.5%, which was significantly better than that of water flooding. The comprehensive index shows that the salt-tolerant polymer meets the technical standards of polymer flooding in low-permeability reservoirs.

Pressure increases significantly after polymer injection. After polymer injection, the polymer solution will first occupy the large-pore water-flooded layer. Due to the retention of macromolecular polymers in the formation pores caused by adsorption and trapping, the permeability of the large-pore water-flooded layer is reduced, and the injection pressure is increased, so that the solution is more in the middle- and low-permeability layers, and the swept volume is increased [46]. In reservoirs with poor connectivity and low permeability, macromolecular polymer solutions have difficulty entering the reservoir; the starting pressure of the reservoir increases, and the injection pressure increases. The molecular weight of the polymer is low, and the pressure increases so that it can smoothly enter the low-permeability rock formation and increase the swept volume of the low-permeability reservoir [47].

3.2. Surfactant Performance Evaluation

3.2.1. Salt-Tolerant Surfactant Screening

The crude oil in the block belongs to conventional light, low-condensation and low-acid crude oil. The hydrogen–carbon ratio is high. The content of resin and asphaltene is about 11%. The formation water type is $NaHCO_3$ type. The total salinity is 24.6 g/L, which belongs to medium to high salinity. The content of calcium and magnesium ions is medium. It has the characteristics of low-reservoir permeability, high salinity of formation water, and injected water. The surface-active agent screening includes three categories: anionic surface-active agent, nonionic surface-active agent, and zwitterionic surface-active agent. The anion surfactant can regulate the resistance to calcium and magnesium ions; when the temperature of the nonionic surfactant is high, the solubility becomes worse; the emulsifying ability is strong, but the emulsification is not controllable. The zwitterionic surfactant has good salt and temperature resistance and high interfacial activity. The pore radius of the low-permeability reservoir is small, and the adsorption capacity of surfactant is relatively large, which will have a great impact on the performance of the surfactant. It is necessary for the surfactant to have strong anti-adsorption ability and a certain salt tolerance. Therefore, ten surfactants were screened out.

The surfactant concentration was 0.25%, and the solution was formation water. The results are shown in Table 8. The interfacial tension of B (CAS68603-42-9) was the lowest (0.0058 mN/m), showing excellent interfacial activity. A (CAS581089-19-2) followed by 0.0081 mN/m. The effect of other surfactants on reducing interfacial tension is relatively weak. Therefore, A was selected as the main agent and B as the auxiliary agent to carry out the compound optimization research. Subsequent evaluation was carried out with the compound system.

Table 8. Oil–Water Interfacial Tension Scanning Results.

Surfactant	**A**	**B**	**C**	**D**	**E**	**F**
σ, mN/m	0.0081	0.0058	0.056	0.042	0.0525	0.302
Surfactant	**G**	**H**	**I**	**J**	**K**	**L**
σ, mN/m	0.628	0.177	0.292	0.167	0.019	0.0226

In order to further enhance the synergistic effect of surfactant, the compounding experiments of A and B with different ratios at a total concentration of 0.25% were designed. The results are shown in Table 9, and their effects on the oil–water interfacial tension were systematically investigated. The ratio range A:B = 10:0 to 0:10 (a total of 11 groups) was used to test the oil–water interfacial tension. When A:B = 7:3, the oil–water equilibrium interfacial tension decreased to 9×10^{-4} mN/m. Compared with the use of A or B alone,

the interfacial tension decreased further after compounding, indicating that there was an obvious synergistic effect; it has good emulsification and washing oil ability. Based on the experimental results, the surfactant system was determined to be the combination of the main agent A and the auxiliary agent B, and the best compounding ratio was A:B = 7:3.

Table 9. Determination of the Optimal Mixing Ratio of AB Agents.

A:B	10:0	9:1	8:2	7:3	6:4	5:5	4:6	3:7	2:8	1:9	0:10
σ, mN/m	0.0081	0.0042	0.0017	0.0009	0.0013	0.0028	0.0033	0.0036	0.0043	0.0051	0.0058

3.2.2. Salt-Tolerance Evaluation

The change of the interfacial tension of surfactant under different salt concentration conditions is shown in Figure 5. The total salinity of formation water is within the experimental test range (0.5~3%). The interfacial tension of the surfactant system is stable and up to standard in this salinity range. It shows that the salt tolerance range of the surfactant system completely covers the salinity change range of the reservoir, showing promising application prospects.

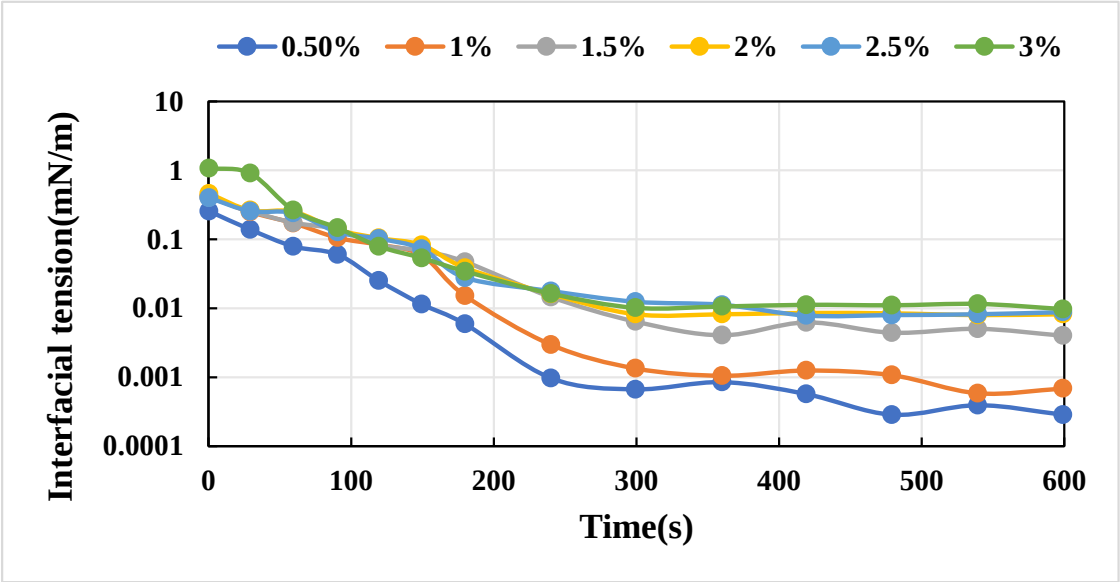

Figure 5. The change of interfacial tension under different salt concentrations and different times.

3.2.3. Emulsifying Evaluation of Surfactant

Three groups of surfactant emulsification ability determination experiments were carried out. The experimental results are shown in Table 10. The surfactant system has a high emulsifying power (average 87.53%), which can effectively promote oil–water mixing and improve crude oil fluidity. The emulsion stability was moderate (average 79.17%). The comprehensive index of emulsification reached 83.24%. The comprehensive performance was excellent and met the needs of field application. Thanks to the excellent interfacial activity and emulsification performance, the surfactant system can effectively remove the residual oil film attached to the pore wall during the oil displacement process and enhance the oil recovery.

Table 10. Evaluation Results of Surfactant Emulsification Performance.

Experiment Number	Emulsifiability (%)	Emulsion Stability (%)	Emulsification Comprehensive Index (%)
1	85.60	78.63	82.04
2	87.30	79.21	83.16
3	89.70	79.66	84.53
Average value	87.53	79.17	83.24

When zwitterionic surfactant and nonionic surfactant are combined, the molecules of different polarities are attracted to each other when adsorbed at the gas–liquid interface, reducing the repulsion between the same molecules, making the adsorption layer more closely arranged, significantly reducing the critical micelle concentration and surface tension of the system. The surface activity is stronger than when one of them is used alone, adapting to the high-salt and low-permeability reservoir in Changqing [48].

3.2.4. Evaluation of Surfactant Displacement Effect

The core displacement experiment was carried out for the surfactant system. The density of crude oil is 0.85 g/mL, the salinity of formation water is 24,600 mg/L, the injection water of water flooding is formation water, the chemical flooding is 0.20% surfactant formation water solution, the experimental temperature is 40 °C, and the injection rate is 0.05 mL/min. The experimental core is the No. 5 core, and the permeability is 20.11 mD. The experimental results are shown in Figure 6. After the surfactant was injected, the oil displacement efficiency increased from 45.71% to 51.43%, indicating that the surfactant effectively released part of the bound oil. After subsequent water flooding, the final total oil displacement efficiency reached 61.33%; the system improves the oil displacement efficiency by 15.62% on the basis of water flooding.

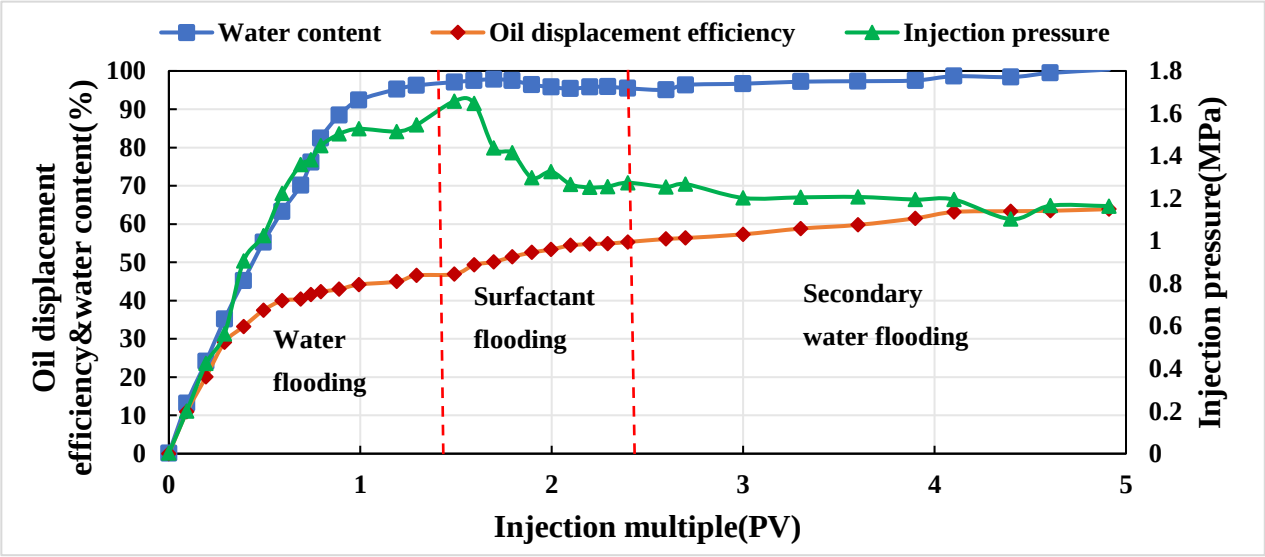

Figure 6. Experimental results of natural homogeneous core displacement.

3.3. Performance Evaluation of SP System

3.3.1. Viscosity and Interfacial Tension of the Composite Systems

The polymer and surfactant were compounded to form a new SP system. The compatibility of the system was evaluated by measuring the viscosity change and interfacial tension of the SP system. The experimental results are shown in Table 11 and Figure 7. It

can be seen from the performance evaluation results of the SP system that the compatibility of polymer and surfactant is good, and the interfacial tension of the SP system can still maintain an ultra-low state. The viscosity retention rate is high, and the surfactant promoted the partial association of the polymer, increased the viscosity of the polymer solution by 5.8%, and improved the oil displacement capacity of the system.

Table 11. Performance evaluation of SP system.

Interfacial Tension (mN/m)		Viscosity (mPa·s)	
Surfactant	**Surfactant + Polymer**	**Surfactant**	**Surfactant + Polymer**
0.0042	0.007	23.9	25.3

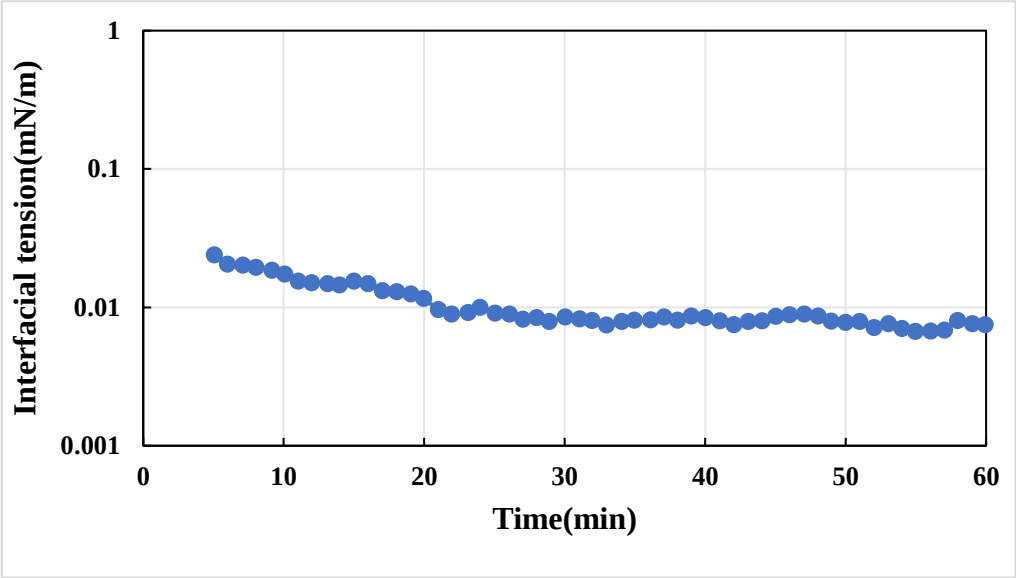

Figure 7. Interfacial tension of SP system.

The carboxylate and sulfonate anion sites on the AA/AMPS/AM terpolymer chain can form a stable electrostatic adsorption with the positive charge of the zwitterionic EHSB head. At the same time, the hydrophobic side chain of the polymer molecular chain will be intertwined with the long erucic acid hydrophobic carbon chain of EHSB and the coconut oil hydrophobic chain of CDEA, which improves the shear stability and avoids the rapid attenuation of viscosity during displacement. The sulfonate group can form a dense hydration layer, which cooperates with the polar head of EHSB sulfobetaine to shield the charge neutralization effect of high valence cations such as Na^+ and Ca^{2+} on the polymer molecular chain in the reservoir, so as to avoid the loss of viscosity caused by the curling of the polymer chain [49,50].

3.3.2. Evaluation of Composite Systems Displacement Effect

The average core displacement experiment was carried out for the SP system. The crude oil density was 0.85 g/mL, the formation water salinity was 24,600 mg/L, the water flooding injection water was formation water, the chemical flooding was 0.20% SP system formation water solution, the experimental temperature was 40 °C, and the injection rate was 0.05 mL/min. The experimental core is the No. 6 core, and the permeability is 37.28 mD. The experimental results are shown in Figure 8. After injection of SP system, the oil displacement efficiency increased from 45.5% to 59.8%, indicating that the SP system effectively released part of the bound oil. After subsequent water flooding, the final total

oil displacement efficiency reached 65%; the SP system improves the oil displacement efficiency by 19.50% on the basis of water flooding.

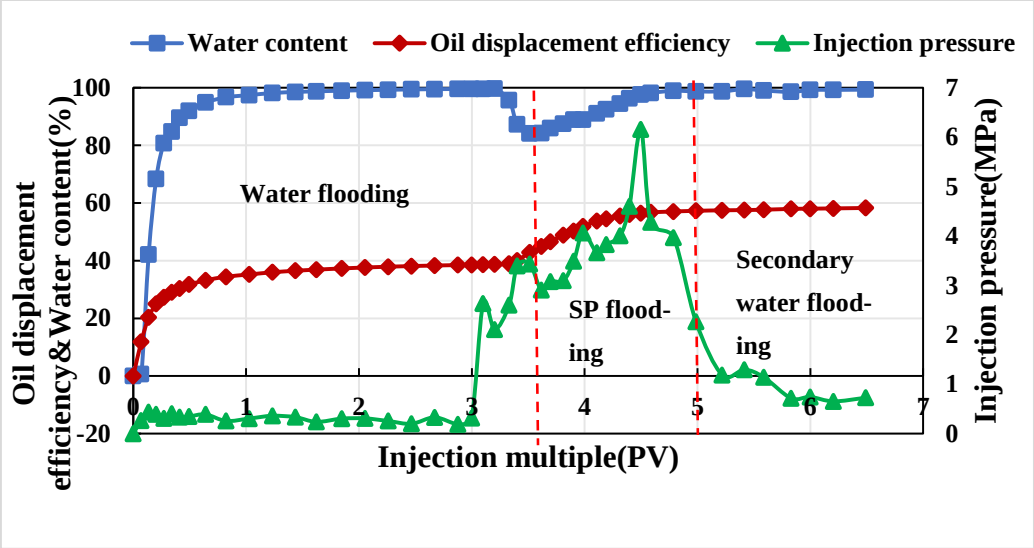

Figure 8. Homogeneous core SP system displacement experiment results.

In order to evaluate the adaptability and oil displacement efficiency of the SP system under the condition of actual reservoir heterogeneity, the condition of permeability ratio of 3.91 is set to simulate different degrees of reservoir heterogeneity. The density of crude oil is 0.85 g/mL, the salinity of formation water is 24,600 mg/L, the injection water of water flooding is formation water, the chemical flooding is 0.20% SP system formation water solution, the experimental temperature is 40 °C, and the injection rate is 0.05 mL/min. The experimental cores are the No. 7 and No. 8 cores, and the No. 7 core is a low-permeability core with a permeability of 35.9 mD; core No. 8 is a high-permeability core with a permeability of 140.4 mD. The experimental results are shown in Figure 9. The water flooding recovery rate is 37.92%, the total recovery rate is 57.88%, and the recovery rate is 19.96% higher than that of water flooding. The SP system improves the oil recovery rate by nearly 20%, indicating that it has good flooding ability and sweep efficiency.

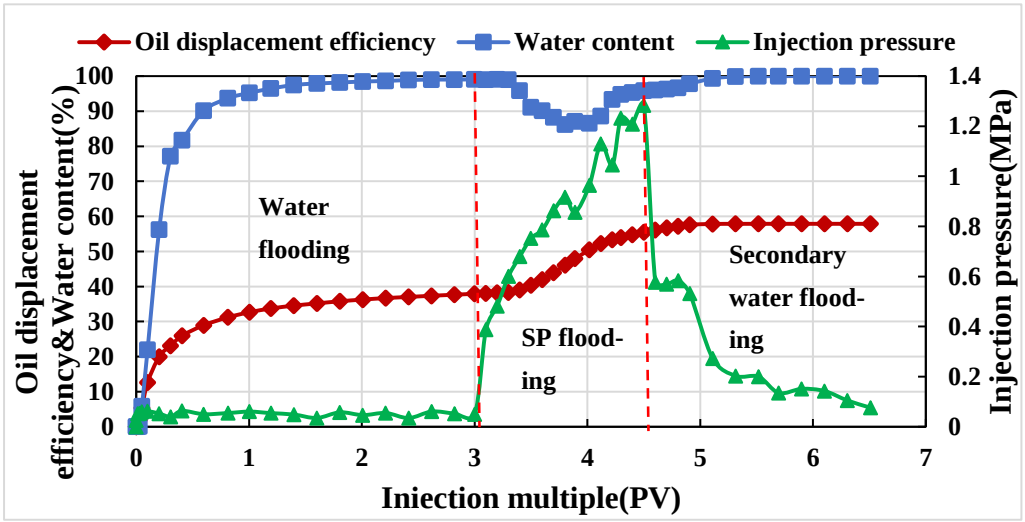

Figure 9. Permeability ratio 3.91 Heterogeneity Displacement Experiment Results.

The displacement experiments were carried out on high-permeability and low-permeability cores separately. The experimental results are shown in Figure 10, but the oil displacement efficiency of low-permeability cores was higher. The difference in oil displacement efficiency between high-permeability and low-permeability cores was small (only about 2.21%), indicating that the binary system has good sweep efficiency in heterogeneous media.

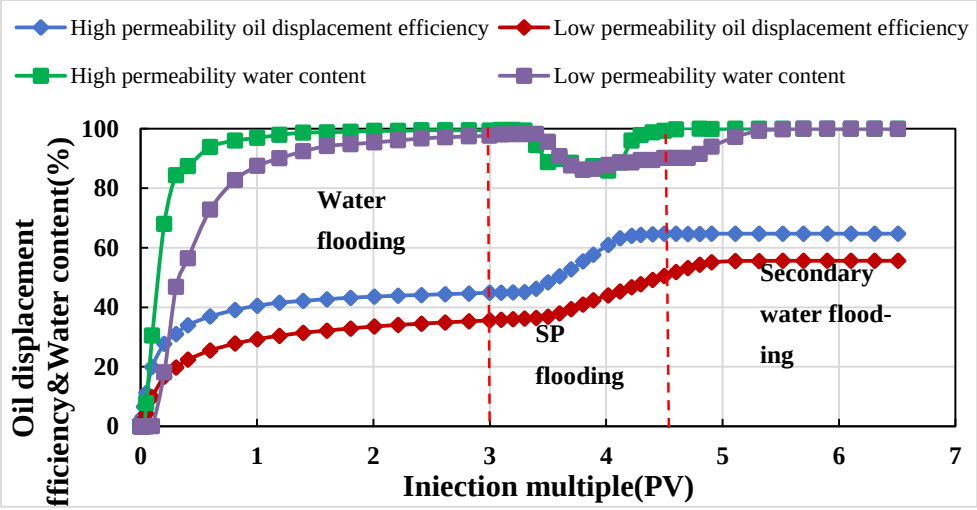

Figure 10. Permeability ratio 3.91 Single Core Displacement Experiment Results.

3.3.3. Parallel Core Displacement Experiment Shunt Flow Experimental Evaluation

The proportion of the partial flow of the parallel core is shown in Figure 11. In the water flooding stage, the high permeability core makes more water enter it by virtue of the permeability advantage, and the amount of the expelled liquid accounts for 0.8 of the total liquid volume. With the addition of the broken chemical agent, the proportion of the expelled liquid volume of the high-permeability and low-permeability core does not change. Furthermore, the low-permeability liquid production gradually increases, accounting for more than half of the total liquid production. During the secondary water flooding, the proportion of the high-permeability and low-permeability liquid volume appears alternately, and there is no obvious law. The experimental results show that after the addition of the SP system, the proportion of remaining oil recovery in low-permeability cores is significantly increased, and the system is suitable for the displacement of low-permeability reservoirs.

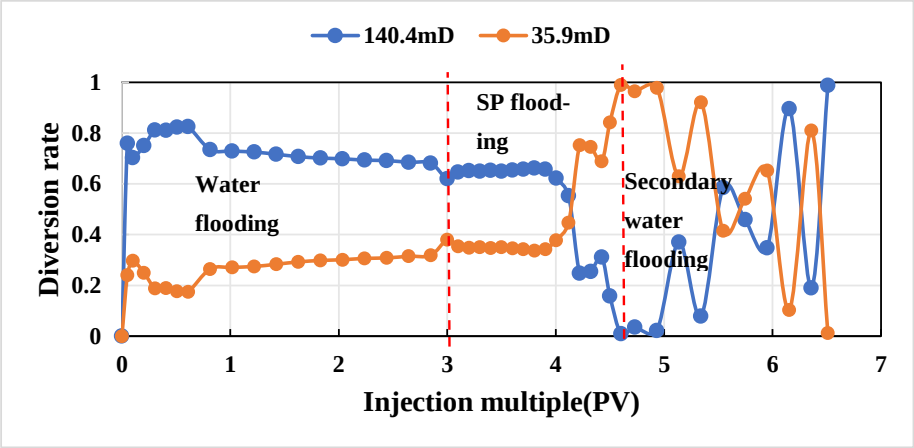

Figure 11. High-permeability and low-permeability core flow ratio diagram.

3.4. Economic Analysis of SP System

The main polymer of the SP flooding system in Changqing Oilfield is polyacrylamide, and the main surfactant is customized betaine surfactant (such as Coco-alkyldimethy). In this paper, the polymer is a terpolymer of AA, AMPS, and AM, and the surfactant is a compound system of EHSB and CDEA. The cost of all reagents is shown in Table 12.

Table 12. Old and new chemical agent material cost comparison table.

	Polymer Prices ($)	Surfactant Price ($)
Old chemical agents	1930.5/ton	1859/ton
New chemical agents	1510.08/ton	2059.2/ton

It can be seen from the table that the price of the ternary polymer synthesized in this paper is USD 1510.08 per ton, which is USD 420.42 less than the cost of HPAM currently used in Changqing. The cost of surfactant compounding in this paper is USD 200.2 higher than that of the surfactant currently used in Changqing. However, the surfactants and polymers used in this paper have good performance and still have good performance at low concentrations. The synthesis route of the ternary polymer involved in this paper is relatively mature, and the cost of industrial preparation of the polymer is low. The synthesis of polymer by aqueous solution polymerization can directly use the sewage produced by Changqing Oilfield and further reduce the cost. Therefore, compared with the traditional system of Changqing Oilfield, the SP system can not only improve the performance, but also save a certain cost, which is suitable for long-term application in Changqing Oilfield.

4. Conclusions

(1) The viscosity of the polymer was determined according to the formation conditions, and acrylic acid/polyacrylamide/2-acryloylamino-2-methyl-1-propanesulfonic acid was selected. The polymer had good filtration characteristics. The viscosity remained stable at the formation temperature, which could increase the oil displacement efficiency by 14.5%.

(2) The interfacial tension of various surfactants was scanned, and the surfactant system with A:B of 7:3 was selected. It has good adsorption resistance, and the interfacial tension can reach 0.0009 mN/m. It can improve the oil displacement efficiency by more than 10% on the basis of water flooding, and the effect of improving oil recovery is obvious.

(3) The polymer–surfactant binary system was constructed. The surfactant promotes the partial association of the polymer and improves the oil displacement capacity of the system, which can improve the oil displacement efficiency by 19.5% in the natural core displacement experiment. In the parallel core experiment, the recovery rate can be improved by 19.96%. The results of fractional flow show that the swept volume of the low-permeability reservoir increases significantly.

Author Contributions: Data curation, Y.S.; Methodology, X.Q., G.Y., K.T.; Investigation, W.X.; Formal analysis, Q.T., X.K.; Software, L.L.; Validation, H.G., Q.W., H.H.; Writing—original draft, L.C. All authors have read and agreed to the published version of the manuscript.

Funding: This research was funded by China National Major Science & Technology Project "Enhanced oil recovery technology integrated demonstration for low/ultra-low permeability and high water-cut oil reservoirs" (No. 2025ZD1407200).

Data Availability Statement: The original contributions presented in this study are included in the article.

Acknowledgments: Thanks to the experts of Changqing Oilfield Exploration and Development Research Institute for the advice and guidance in this study. Thanks to Hongze Wu, Xinyi Sun, Ziang Jin, and Shihao Sun of Changzhou University for the help with the experiment.

Conflicts of Interest: Authors Yangnan Shangguan, Xuefeng Qu, Guowei Yuan, Weiliang Xiong, Kang Tang, Qianqian Tian, Lei Liu, Hua Guan, Qi Wang, Xingmei Kang were employed by the Exploration & Development Research Institute, Changqing Oilfield Company. The remaining authors declare that the research was conducted in the absence of any commercial or financial relationships that could be construed as a potential conflict of interest. The company had no role in the design of the study; in the collection, analyses, or interpretation of data; in the writing of the manuscript, or in the decision to publish the results.

References

1. Song, Y.; Li, Z.; Jiang, Z.; Luo, Q.; Liu, D.; Gao, Z. Progress and development trend of unconventional oil and gas geological research. *Pet. Explor. Dev.* **2017**, *44*, 675–685. [CrossRef]
2. Wang, H.J.; Ma, F.; Tong, X.G.; Liu, Z.; Zhang, X.; Wu, Z.; Li, D.; Wang, B.; Xie, Y.; Yang, L. Assessment of global unconventional oil and gas resources. *Pet. Explor. Dev.* **2016**, *43*, 925–940. [CrossRef]
3. Das, A.; Nguyen, N.; Nguyen, Q.P. Low tension gas flooding for secondary oil recovery in low-permeability, high-salinity reservoirs. *Fuel* **2020**, *264*, 116601. [CrossRef]
4. Leitner, W. Reactions in supercritical carbon dioxide (sc CO_2). In *Modern Solvents in Organic Synthesis*; Springer: Berlin/Heidelberg, Germany, 1999; pp. 107–132.
5. Yang, Z.; Li, M.; Peng, B.; Lin, M.; Dong, Z. Dispersion property of CO_2 in oil. 1. Volume expansion of CO_2+ alkane at near critical and supercritical condition of CO_2. *J. Chem. Eng. Data* **2012**, *57*, 882–889. [CrossRef]
6. Li, X.; Ross, D.A.; Trusler, J.P.M.; Maitland, G.C.; Boek, E.S. Molecular dynamics simulations of CO_2 and brine interfacial tension at high temperatures and pressures. *J. Phys. Chem. B* **2013**, *117*, 5647–5652. [CrossRef]
7. Ping, G.; Miao, L. A study on the miscible conditions of CO_2 injection in low-permeability sandstone reservoirs. *Oil Gas Geol* **2007**, *28*, 687–692.
8. Wang, R.; Zhang, Y.; Lyu, C.; Lun, Z.; Cui, M.; Lang, D. Displacement characteristics of CO_2 flooding in extra-high water-cut reservoirs. *Energy Geosci.* **2024**, *5*, 100115. [CrossRef]
9. Ahmad, W.; Vakili-Nezhaad, G.; Al-Bemani, A.S.; Al-Wahaibi, Y. Experimental determination of minimum miscibility pressure. *Procedia Eng.* **2016**, *148*, 1191–1198. [CrossRef]
10. Wang, Y.J.; Song, X.M.; Tian, C.B.; Shi, C.; Li, J.; Hui, G.; Hou, J.; Gao, C.; Wang, X.; Liu, P. Dynamic fractures are an emerging new development geological attribute in water-flooding development of ultra-low permeability reservoirs. *Pet. Explor. Dev.* **2015**, *42*, 247–253. [CrossRef]
11. Veatch, J.R.; McMurray, M.A.; Nelson, Z.W.; Gottschling, D.E. Mitochondrial dysfunction leads to nuclear genome instability via an iron-sulfur cluster defect. *Cell* **2009**, *137*, 1247–1258. [CrossRef]
12. Wang, Y.; Shang, Q.; Zhou, L.; Jiao, Z. Utilizing macroscopic areal permeability heterogeneity to enhance the effect of CO_2 flooding in tight sandstone reservoirs in the Ordos Basin. *J. Pet. Sci. Eng.* **2021**, *196*, 107633. [CrossRef]
13. Zhang, Y.; Gao, M.; You, Q.; Fan, H.; Li, W.; Liu, Y.; Fang, J.; Zhao, G.; Jin, Z.; Dai, C. Smart mobility control agent for enhanced oil recovery during CO_2 flooding in ultra-low permeability reservoirs. *Fuel* **2019**, *241*, 442–450. [CrossRef]
14. Wei, J.; Zhou, J.; Li, J.; Zhou, X.; Dong, W.; Cheng, Z. Experimental study on oil recovery mechanism of CO_2 associated enhancing oil recovery methods in low permeability reservoirs. *J. Pet. Sci. Eng.* **2021**, *197*, 108047. [CrossRef]
15. Xiao, P.; Yang, Z.; Wang, X.; Xiao, H.; Wang, X. Experimental investigation on CO_2 injection in the Daqing extra/ultra-low permeability reservoir. *J. Pet. Sci. Eng.* **2017**, *149*, 765–771. [CrossRef]
16. Shen, H.; Yang, Z.; Li, X.; Peng, Y.; Lin, M.; Zhang, J.; Dong, Z. CO_2-responsive agent for restraining gas channeling during CO_2 flooding in low permeability reservoirs. *Fuel* **2021**, *292*, 120306. [CrossRef]
17. Zhang, J.; Seyyedi, M.; Clennell, M.B. Molecular dynamics simulation of transport and structural properties of CO_2–alkanes. *Energy Fuels* **2021**, *35*, 6700–6710. [CrossRef]
18. Rellegadla, S.; Prajapat, G.; Agrawal, A. Polymers for enhanced oil recovery: Fundamentals and selection criteria. *Appl. Microbiol. Biotechnol.* **2017**, *101*, 4387–4402. [CrossRef] [PubMed]
19. Wever, D.A.Z.; Picchioni, F.; Broekhuis, A.A. Polymers for enhanced oil recovery: A paradigm for structure–property relationship in aqueous solution. *Prog. Polym. Sci.* **2011**, *36*, 1558–1628. [CrossRef]
20. Wu, G.; Yu, L.; Jiang, X. Synthesis and properties of an acrylamide-based polymer for enhanced oil recovery: A preliminary study. *Adv. Polym. Technol.* **2018**, *37*, 2763–2773. [CrossRef]

21. Khakpour, H.; Abdollahi, M. Rheological properties of acrylamide/butyl acrylate/2-acrylamido-2-methyl-1-propane sulfonic acid co-and terpolymers synthesized by heterogeneous and micellar methods. *Polym. Bull.* **2017**, *74*, 5145–5161. [CrossRef]
22. Evani, S. Water-Dispersible Hydrophobic Thickening Agent. U.S. Patent 4432881, 20 February 1984.
23. Mohan, K. Alkaline surfactant flooding for tight carbonate reservoirs. In Proceedings of the SPE Annual Technical Conference and Exhibition, New Orleans, LA, USA, 4–7 October 2009; SPE: Richardson, TX, USA, 2009; SPE-129516-STU.
24. Hincapie, R.E.; Rock, A.; Wegner, J.; Ganzer, L. Oil mobilization by viscoelastic flow instabilities effects during polymer EOR: A pore-scale visualization approach. In Proceedings of the SPE Latin America and Caribbean Petroleum Engineering Conference, Buenos Aires, Argentina, 17–19 May 2017; SPE: Richardson, TX, USA, 2017; D011S002R002.
25. Foster, W.R. A low-tension waterflooding process. *J. Pet. Technol.* **1973**, *25*, 205–210. [CrossRef]
26. Ning, J.; Wei, B.; Mao, R.; Wang, Y.; Shang, J.; Sun, L. Pore-level obscrvations of an alkali-induced mild O/W emulsionflooding for economic enhanced oil recovery. *Energy Fuels* **2018**, *32*, 10595–10604. [CrossRef]
27. Dong, M.; Ma, S.; Liu, Q. Enhanced heavy oil recovery through interfacial instability: A study ofchemical flooding for Brintnell heavy oil. *Fuel* **2009**, *88*, 1049–1056. [CrossRef]
28. An, Y.X.; Yao, X.T.; Zhong, J.P.; Pang, S.; Xie, H. Enhancement of oil recovery by surfactant-polymer synergy flooding: A review. *Polym. Polym. Compos.* **2022**, *30*, 09673911221145834. [CrossRef]
29. Holley, S.M.; Cayias, J.L. Design, operation, and evaluation of a surfactant/polymer field pilot test. *SPE Reserv. Eng.* **1992**, *7*, 9–14. [CrossRef]
30. Avwioroko, J.; Taiwo, O.; Mohammed, I.; Dala, J.; Olafuyi, O. A Laboratory Study of ASP Flooding on Mixed Wettability for Heavy Oil Recovery Using Gum Arabic as a Polymer. In Proceedings of the SPE Nigeria Annual International Conference and Exhibition, Lagos, Nigeria, 5–7 August 2014.
31. Liu, J.; Zhang, K.; Huang, L.; Li, H. Research on Factors Influencing Weak Alkali Surfactant Polymer Flooding System. *Chem. Technol. Fuels Oils* **2021**, *57*, 724–731. [CrossRef]
32. Zaitoun, A.; Kohler, N. The Role of Adsorption in Polymer Propagation Through Reservoir Rocks. In Proceedings of the SPE International Symposium on Oilfield Chemistry, San Antonio, TX, USA, 4–6 February 1987; Society of Petroleum Engineers: Richardson, TX, USA, 1987.
33. Zhang, J.; Ge, D.; Wang, X.; Wang, W.; Cui, D.; Yuan, G.; Wang, K.; Zhang, W. Influence of Surfactant and Weak-Alkali Concentrations on the Stability of O/W Emulsion in an Alkali-Surfactant–Polymer Compound System. *ACS Omega* **2021**, *6*, 5001–5008. [CrossRef] [PubMed]
34. Sorbie, K.S. *Polymer-Improved Oil Recovery*; Springer Science & Business Media: Dordrecht, The Netherlands, 2013.
35. Chan, A.F.; Parmley, J.P. Gravel sizing criteria for sand control and productivity optimization. II—Evaluation of the long-termed stability. In Proceedings of the SPE Formation Damage Control Symposium, Lafayette, Louisiana, 26–27 February 1992; pp. 37–54. [CrossRef]
36. Wei, J.; Chen, Y.; Zhou, X.; Wang, L.; Fu, P.; Yakushev, V.; Khaidina, M.; Zhang, D.; Shi, X.; Zhou, R. Experimental studies of surfactant-polymer flooding: An application case investigation. *Int. J. Hydrogen Energy* **2022**, *47*, 32876–32892. [CrossRef]
37. Al-Murayri, M.T.; Hassan, A.A.; AlAbdullah, M.B.; Abdulrahim, A.M.; Marlière, C.; Hocine, S.; Tabary, R.; Suzanne, G.P. Surfactant/polymer flooding: Chemical-formulation design and evaluation for Raudhatain lower Burgan Reservoir, Kuwait. *SPE Reserv. Eval. Eng.* **2019**, *22*, 923–940. [CrossRef]
38. Sidorovskaya, E.A.; Adakhovskij, D.S.; Tret, N.Y.; Panicheva, L.P.; Volkova, S.S.; Turnaeva, E.A. Integrated laboratory studies when optimizing surfactant-polymer formulations for oil deposits in Western Siberia. *Нефть и газ = Oil Gas Stud.* **2020**, 107–118. [CrossRef]
39. Le Van, S.; Chon, B.H. Numerical studies on the effects of various complicated barrier configurations on sweep efficiency in surfactant/polymer flooding. *J. Ind. Eng. Chem.* **2016**, *38*, 200–210. [CrossRef]
40. Suzanne, G.; Soltani, A.; Charonnat, S.; Delamaide, E. Use of numerical simulation enhanced by machine learning techniques to optimize chemical EOR application. In Proceedings of the Abu Dhabi International Petroleum Exhibition and Conference, Abu Dhabi, United Arab Emirates, 31 October–3 November 2022; SPE: Richardson, TX, USA, 2022; D021S059R003.
41. Yuan, L.; Wu, Y.; Fan, Q.; Li, P.; Liang, J.; Wang, Z.; Li, R.; Shi, L. Spatial distribution, composition, and source analysis of petroleum pollutants in soil from the Changqing Oilfield, Northwest China. *Mar. Pollut. Bull.* **2022**, *185*, 114338. [CrossRef] [PubMed]
42. Yang, H.; Liu, X.; Huang, D.; Lan, Y.; Wang, S. Natural gas exploration and development in Changqing Oilfield and its prospect in the 13th Five-Year Plan. *Nat. Gas Ind. B* **2016**, *3*, 291–304. [CrossRef]
43. Cui, C.; Zhou, Z.; He, Z. Enhance oil recovery in low permeability reservoirs: Optimization and evaluation of ultra-high molecular weight HPAM/phenolic weak gel system. *J. Pet. Sci. Eng.* **2020**, *195*, 107908. [CrossRef]
44. Xue, D.; Wu, L.; Gao, R.; Cao, Y.; Zhao, C.; Liu, Q.; Li, Y.; Tang, Y.; Slaný, M.; Chen, G. Synthesis and performance study of the fracturing thickener P (AM/AA/AMPS/NVP/DMAAC-16) for rapid fluid preparation. *J. Mol. Liq.* **2025**, *435*, 128113. [CrossRef]

45. Ding, X.; Zhang, G.; Wang, X.; Xin, K.; Wang, F.; Zhou, T.; Wang, X.; Zhang, Z. Preparation of thickened P (AA-AMPS) copolymers by inverse emulsion polymerization and evaluation of fracturing and oil flooding performance. *J. Mol. Liq.* **2024**, *415*, 126400. [CrossRef]
46. Lin, Z.; Lu, X.; Zhang, B.; Liu, W.; Ding, B.; Chang, Y.; Rui, Z.; Zeng, F.; Zhang, S. Feasibility study of CO_2-based cyclic solvent injection and polymer flooding alternation process to enhance heavy oil recovery. *J. CO_2 Util.* **2025**, *102*, 103276. [CrossRef]
47. Farhadinia, M.A.; Mohanty, K.K. Heavy oil recovery using hot polymer flooding: Simulation studies on mechanisms and injection patterns. *Fuel* **2026**, *405*, 136435. [CrossRef]
48. Zhang, S.; Wang, F.; Tan, B.; Wang, Y.; Liu, P.; Kim, T.; Guo, L.; Han, X.; Liu, R. Enhanced particle removal ability of two representative nonionic surfactants: A reasonable interpretation based on DFT and coarse-grained molecular dynamics methods. *J. Mol. Liq.* **2024**, *413*, 125984. [CrossRef]
49. Zhao, H.; Kang, W.; Yang, H.; Huang, Z.; Zhou, B.; Sarsenbekuly, B. Emulsification and stabilization mechanism of crude oil emulsion by surfactant synergistic amphiphilic polymer system. *Colloids Surf. A Physicochem. Eng. Asp.* **2021**, *609*, 125726. [CrossRef]
50. Varel, F.T.; Dai, C.; Shaikh, A.; Li, J.; Sun, N.; Yang, N.; Zhao, G. Chromatography and oil displacement mechanism of a dispersed particle gel strengthened Alkali/Surfactant/Polymer combination flooding system for enhanced oil recovery. *Colloids Surf. A Physicochem. Eng. Asp.* **2021**, *610*, 125642. [CrossRef]

Disclaimer/Publisher's Note: The statements, opinions and data contained in all publications are solely those of the individual author(s) and contributor(s) and not of MDPI and/or the editor(s). MDPI and/or the editor(s) disclaim responsibility for any injury to people or property resulting from any ideas, methods, instructions or products referred to in the content.